steel research international

Effect of Material Processing and Imposed Mechanical Stress on the Magnetic, Mechanical, and Microstructural Properties of High-Silicon Electrical Steel

Nora Leuning,* Simon Steentjes, Kay Hameyer, Markus Schulte, and Wolfgang Bleck*

This paper investigates the detrimental effect of material processing steps on magnetic, mechanical, and microstructural properties of silicon-alloyed steel. For that purpose, both water jet and guillotine cutting as well as various tensile loadings (elastic and plastic) are studied, which correlate to shape giving processes and mechanical loadings that occur during machine production and operation. Mechanical processing such as guillotine shear cutting induces internal stresses that alter the extrinsic magnetic material properties, such as coercivity and remnant induction. In comparison, water jet cutting causes smaller residual stresses. Particular attention is paid to the effect of magneto-crystalline anisotropy, i.e., the influence of the cutting direction with respect to the rolling direction. In order to examine this further, the influence of internal stresses caused by cutting along and perpendicular to the rolling direction is investigated with the help of single-sheet tester magnetic measurements. Therefore, the induced anisotropy is evaluated. The induced anisotropy due to the cutting technique is related to the stress-dependent magnetostriction constant and the grain alignment during cutting. In order to evaluate the general influence of elastic mechanical loadings applied along or perpendicular to the rolling direction on the magnetic behavior, a single-sheet tester equipped with a tensile loading unit is used. In addition, plastically deformed samples are characterized magnetically.

1. Introduction

Silicon-alloyed steel, referred to as *electrical steel*, is a functional material, necessary for electrical applications such as magnetic cores in rotating electrical machines or transformers. Grain-oriented (GO) grades are tailored for the use in devices, e.g., transformers, where an easy direction of magnetization parallel to the rolling direction is desired, i.e., where magnetic fluxes are solely oriented in one spatial direction. Non-grain-oriented (NGO) grades with preferably isotropic magnetic behavior in all spatial directions in the steel sheet plane are applied in rotating electrical machines. Low losses, high-efficiency, and high-power density are the principal aims for the design of electrical machines and are directly linked to the used core material.[1]

The tailoring of electrical, magnetic, and mechanical properties of electrical steel is generally realized by the following measures. Silicon, as the main alloying element in electrical steel, reduces classical, non-local eddy current losses by raising the electrical resistance significantly.[2–3] However, the cold formability is decreased as a result of the increased silicon content.[4] Additionally, the saturation polarization decreases in consequence of the reduced iron content.[5] Therefore, the silicon content is limited to about 3.5 wt% for general applications. Low contents of inclusions and precipitates are desired to reduce impediments to magnetic domain wall motion and to permit fast grain coarsening during final annealing.[6,7] Thereby, hysteresis losses can be reduced particularly. An optimum grain size of 100–

[*] N. Leuning, S. Steentjes, K. Hameyer
Institute of Electrical Machines, RWTH Aachen University, Schinkelstrasse 4, D-52062 Aachen, Germany
Email: nora.leuning@iem.rwth-aachen.de
M. Schulte, W. Bleck
Steel Institute, RWTH Aachen University, Intzestrasse 1, D-52072 Aachen, Germany
Email: info@iehk.rwth-aachen.de

DOI: 10.1002/srin.201600039

150 μm leads to lowermost losses in high-silicon electrical steels for the commercially important induction of 1.5 T.[8–10] A further measure to limit losses is the application of thin steel sheets stacked together to form the machine core. This is mainly beneficial for the reduction of classical, non-local, eddy current losses occurring at high frequencies.[11]

The production process of electromagnetic energy transducers, such as rotating electrical machines, starting from the raw material, is detrimental to the extrinsic magnetic properties of the magnetic core.[12–14] Sheet metal forming, i.e., blanking and shrinking during machine production are particularly critical to the final magnetic characteristics of the core.[15–18] In contrast to semi-finished material, the adverse influence of the sheet metal forming is irreversible for fully finished products, being directly linked to a drop of efficiency of the electrical machine.[19] Although beneficial for the magnetic behavior, measures to limit losses interfere with the sheet metal forming process.[20] Large grains, small sheet thicknesses, and a limited cold formability lead to relatively poor cutting process results, e.g., undefined cracking mechanisms and fluctuating cutting forces. In addition, magnetic properties of electrical steel are highly susceptible to any form of mechanical stresses, residual stresses, as well as external stresses.[21–23] A severe deterioration of magnetic properties can be observed as a result of different cutting techniques.[24]

The purpose of this paper is the elaboration of the influence of cutting on the magnetic and mechanical properties of high-silicon electrical steel with simultaneous consideration of microstructural characteristics. For that purpose, the guillotine shear cutting is chosen in place of sheet metal blanking which is used for batch production of electrical machines and water jet cutting. This is assumed to be very gentle for magnetic property deterioration and is used for preparation of reference sample sets. In particular, the coupling of magnetic properties to stress fields, i.e., magneto-elastic interaction, is studied characterizing sample sets cut along and transverse to the rolling direction. Therefore, the interdependence of roll magnetic anisotropy and induced anisotropy due to internal stresses is worked out.

In order to disentangle the subtleties of the local magneto-elastic coupling originating from the internal stress distribution, the effect of elastic and plastic deformations on extrinsic magnetic properties is investigated with the help of single-sheet tester measurements.

Again, particular attention is paid to the effect of roll anisotropy.

The experimentally determined correlations between material processing and magnetic properties are indispensable for the accurate prediction of magnetizability and iron losses in electrical machines with the help of simulation tools and substitution of currently used empirical building factors by a physical-based model of the complex magneto-mechanical interactions in core materials.

2. Experimental Section

2.1. Material and Investigation Method

The chosen material under study is a commercially available 0.5-mm thick fully finished electrical steel sheet that contains 0.0024 wt% C, 2.9 wt% Si, 0.2 wt% Mn, and 0.75 wt% Al. Regarding its magnetic and technological properties, it can be classified as M270-50A according to DIN EN 10106:2007. The microstructure of the completely recrystallized material was evaluated on the cross-sectional area parallel to the rolling direction by optical microscope. The average final grain size of the ferritic steel is 119 μm measured by traditional intercept method. The microstructural analysis of the cut surfaces was conducted perpendicular to the direction of cutting. Etching was performed by 3% HNO_3 (Nital). Different specimens were prepared by guillotine cutting or water jet cutting in rolling (RD) and transverse direction (TD).

The characterization of mechanical properties in the as-delivered state and the adjustment of the mechanical preload were performed by Zwick Z100 tensile testing machine with a maximum force of 100 kN equipped with a video extensometer for the contactless strain measurement. The cutting surfaces were investigated by Zeiss Sigma SEM and confocal microscope Nanofocus μsurf explorer. An extraordinary resolution in the range of a few nanometers in the z-direction enabled the determination of the sheet roughness. A microhardness of HV 0.05 was measured with the help of Leitz Durimet hardness tester.

2.2. Magnetic Measurements

A metrological characterization was carried out on a $120 \times 120\,mm^2$ single-sheet tester (SST) which was incorporated into a computer-aided setup according to the international standard IEC 60404–3. For a magnetic characterization under tensile stress, a $100 \times 600\,mm^2$ single-sheet tester, equipped with a tensile and compression loading unit is used, which enables to apply mechanical stresses up to a maximum force of 5 kN. In the course of the magnetic measurements, the spatial direction of magnetic flux and applied tensile stress are collinear (uniaxial loading).

In order to study the influence of an increasing fraction of the cut surface related to the sample volume, different strips widths are cut and taped together with a non-magnetic adhesive tape to ensure a comparable geometry of $120 \times 120\,mm^2$, e.g., two strips of 60 mm, four strips of 30 mm, etc. (**Figure 1**).

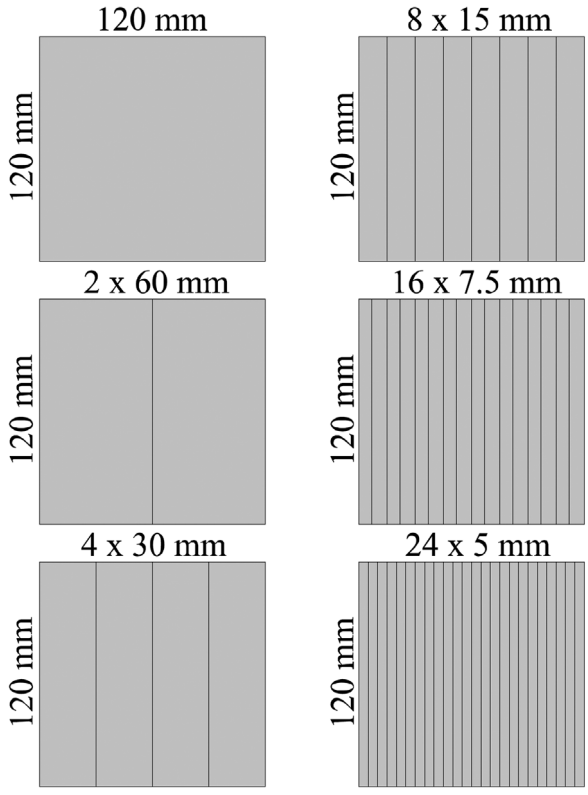

Figure 1. Sample preparation for investigations of different proportions of cut surface per initial sample volume on magnetic behavior. Smaller sample widths result in a higher amount of cut surface per sample set. Samples are cut in rolling direction (RD) and transverse direction (TD) by guillotine and water jet cutting.

3. Results and Discussion

3.1. Effect of Tensile Stress on Magnetic Properties

In order to study the general influence of tensile stresses on the magnetic properties of the 2.9 wt% FeSi electrical steel, two different experimental setups are required to characterize the effect of elastic as well as plastic stresses. For each setup both spatial directions, rolling as well as transverse direction, are studied.

3.1.1. Elastic Tensile Stress in Rolling and Transverse Direction

Figure 2 depicts the resulting hysteresis loops of samples under applied tensile mechanical stresses within the elastic region up to yield strength. Increasing the applied tensile stress in rolling direction shears the hysteresis loops uniformly, i.e., both coercivity H_c as well as the magnetic field strength H which is required to achieve a specific polarization level, increase. Concomitant, the remanence polarization J_r decreases with increasing tensile stress leading to a less distinct slope, i.e., lower relative permeability. Increasing magnetic field strengths to achieve specific polarizations represent inferior electromagnetic applicability for the material, under the investigated stress states. The extrinsic properties coercivity and remanence determine the shape and size of the hysteresis loop to a great extent. Larger values for these properties indicate a larger hysteresis area and thus increased iron losses. The behavior under tensile stresses in rolling direction is monotonic, whereas the behavior in transverse direction shows a non-monotonic effect of increasing tensile stress on the shape of hysteresis loops. Starting from the unloaded state, the hysteresis loops become steeper, i.e., more upright (Figure 2b). The remanence increases while the coercivity decreases. Less magnetic field strength is required to induce a polarization of 1.0 T at 100 Hz.

A further increase of tensile stress shears the hysteresis loop analogous to the samples stressed in rolling direction. For its electromagnetic application, this implies a beneficial effect of small induced tensile stresses.

Figure 3 depicts the characteristic magnetic values (H, H_c, J_r) extracted from the measured hysteresis loops

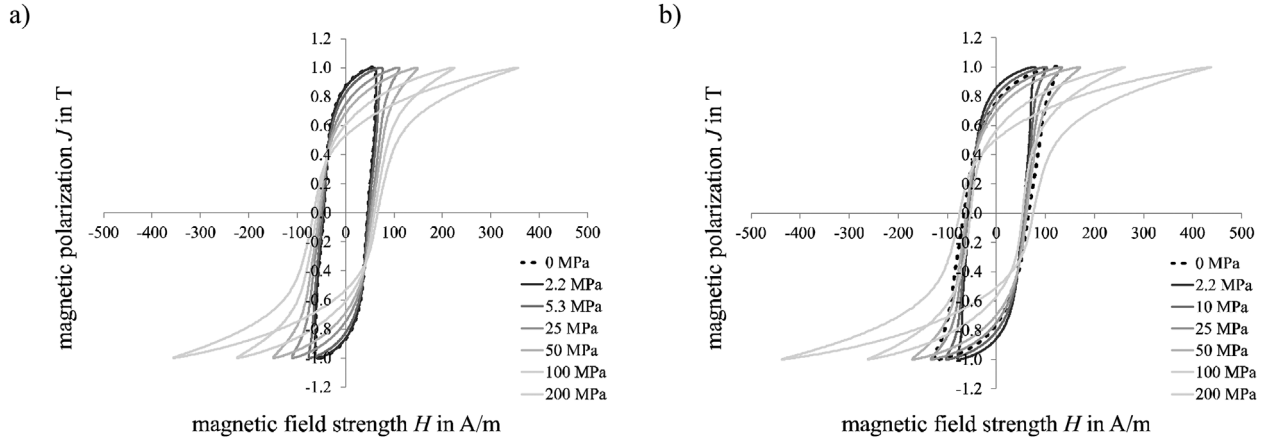

Figure 2. Hysteresis loops at 1.0 T and 100 Hz for increasing elastic tensile stress. Magnetic flux and applied tensile stress are parallel to a) rolling direction and b) transverse direction.

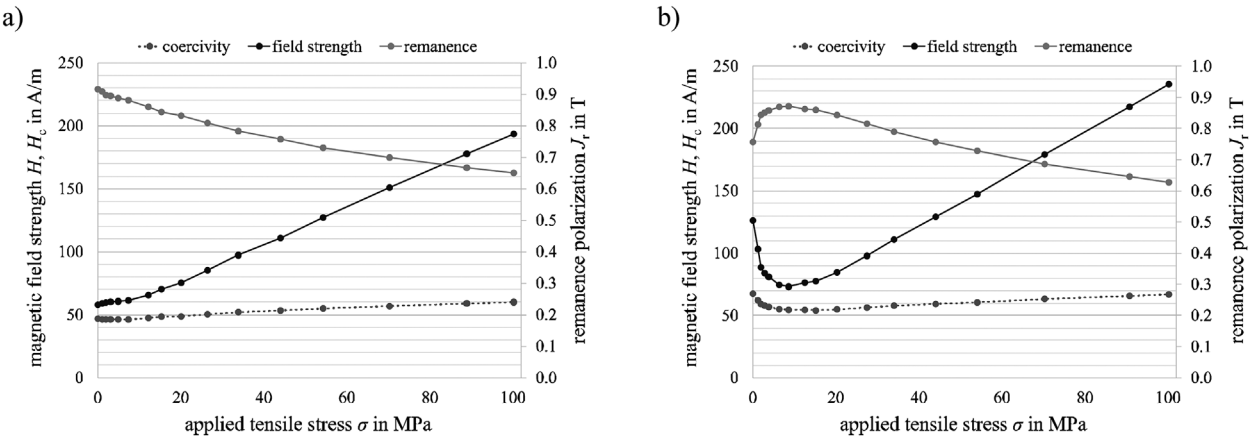

Figure 3. Coercivity, remanence polarization, and magnetic field strength at 1.0 T and 100 Hz for increasing elastic tensile stress. Magnetic flux density and applied tensile stress are parallel to the a) rolling direction and b) transverse direction.

(Figure 2). It is apparent that two distinct sections can be differentiated in rolling direction. For small tensile stresses up to 15 MPa, the characteristic attributes show a minor increase (H, H_c) and decrease (J_r), respectively. Ensuing from 15 MPa onward, the slopes of the curves are constant and larger compared to the first segment. On the contrary, a distinctively different behavior is apparent in transverse direction. For tensile stress levels above 15 MPa, a similar behavior to the rolling direction is observed with a constant increase of coercivity and field strength and decrease of remanence. In comparison to the measured data along the rolling direction, results for transverse direction are inferior. At smaller tensile stress values, the characteristic attributes show pronounced minima and maxima (Figure 3b). For instance, the magnetization behavior is affected beneficially by the application of tensile stresses up to 50 MPa. Beyond this stress level, increasing values of magnetic field strength are required compared to the unloaded state. Therefore, tensile stresses in transverse direction can be beneficial up to a certain threshold value. Nevertheless, the magnetic properties, i.e., magnetizability and iron-loss in rolling direction are in general advantageous at all tensile stress levels compared to the respective stress states in transverse direction.

The effect of an applied tensile elastic stress on the magnetization curve, i.e., on the hysteresis loop of a soft magnetic material can be explained based on the induced magneto-elastic energy that is proportional to the magnetostriction and stress tensor.[25,26] The response of a material to an applied mechanical stress depends on the sign of the tensorial product.[27,28] In order to minimize the magnetic free energy, the domain structure is reorganized.[28] The effect of two elastic strain stages could be related to the effect of micro-yielding which can be measured by a change in Barkhausen noise parameters below $R_{p0.2}$.[11,29] Geometrical necessary dislocations are created close to the grain boundaries to accommodate the strain between grains with different orientations. These dislocations act as pinning sites that reduce the mean free path of the domain wall displacement.[28,30] The effect of two distinct sections within the elastic region is more evidenced in TD, as shown in Figure 3b.

3.1.2. Elastic and Plastic Tensile Stresses in Rolling and Transverse Direction

A further increase of applied tensile stress above $R_{p0.2}$ leads to plastic deformations caused by crystallographic slipping as a result of the dislocation movement. When trying to elaborate the overall effect on the magnetic properties, these need to be accounted in addition to the externally applied elastic stresses. In order to study the effect of plastic deformations on the extrinsic magnetic properties, several samples were plastically deformed on a universal testing machine and subsequently metrologically characterized using a single-sheet tester.

Figure 4 shows the magnetization requirements and coercivity along the entire tensile stress range of elastic and plastic deformations up to tensile strength. Three stress levels between tensile and yield strength were applied for rolling (Figure 4a) as well as the transverse direction (Figure 4b): 470, 500, and 530 MPa. This results in different plastic strains for RD and TD. The respective stress and strain relations are listed in **Table 1**.

Mechanical tensile stresses below yield strength lead to homogenous elastic elongation of the whole specimen. When exceeding the yield strength, the applied stress causes a rising dislocation density which results in the plastic deformation of the specimens. Consequently, a significantly steeper slope of the magnetic field strength than in the elastic region can be observed. This behavior can be explained by a deterioration of the domain size and restricted domain mobility. For that reason, the external magnetic field has to be increased to achieve an alignment of an adequate number of domains along the external magnetic field. In the plastic strain domain, the

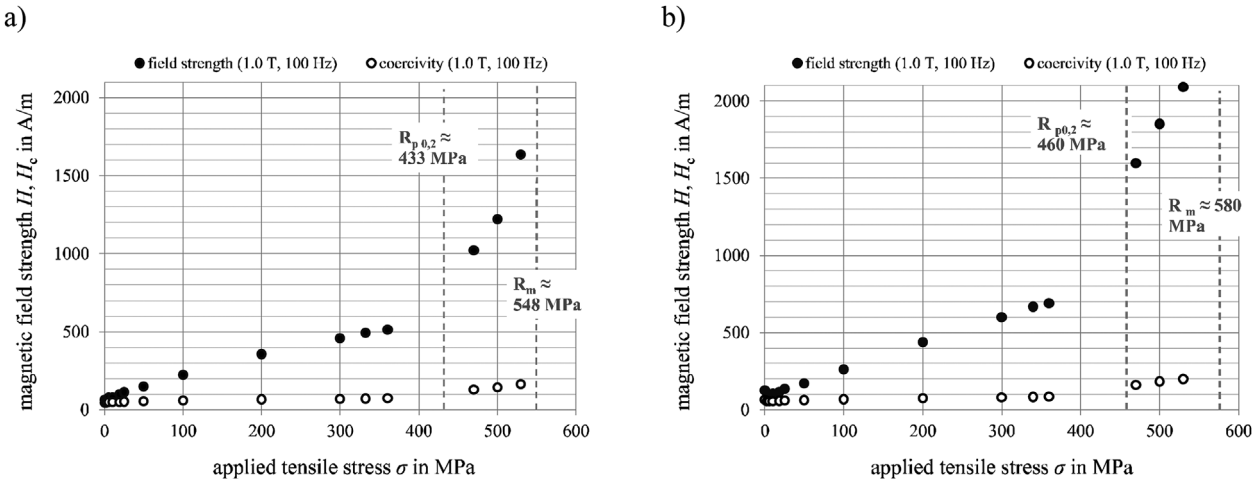

Figure 4. Magnetic field strength and coercivity at increasing tensile stress of elastic and plastic deformations at 1.0 T and 100 Hz. Magnetic measurements and mechanical material parameters (tensile and yield stress) are considered in a) rolling direction and b) transverse direction.

	$\sigma_{mech} = 470$ MPa	$\sigma_{mech} = 500$ MPa	$\sigma_{mech} = 530$ MPa
Rolling direction (RD)	$\varepsilon \approx 4.5\%$	$\varepsilon \approx 6.5\%$	$\varepsilon \approx 12.5\%$
Transverse direction (TD)	$\varepsilon \approx 2.5\%$	$\varepsilon \approx 4.5\%$	$\varepsilon \approx 7.5\%$

Table 1. Stress and resulting strain in rolling and transverse direction under uniaxial tensile stresses above yield strength.

multiplication of dislocations leads to a progressive deterioration of the magnetic behavior.

For the specimens excited parallel to the rolling direction, smaller field strengths are required compared to those in transverse direction. The overall behavior is similar to inferior magnetic properties and the exception of the formerly discussed range of small mechanical stresses.

The effect of internal mechanical stress is clearly evidenced by the results shown in Figure 3 and 4. According to the work of Becker and Kondorski,[31] the inverse of the initial permeability that is related to the required magnetic field strength and the magnetic coercive field strength have a linear relationship with the amount of internal stress.

3.2. Influence of Different Cutting Techniques on Material Properties

3.2.1. Cut Surface Characteristics

At first, a detailed study of the influence of the cutting process on the microstructure and surface morphology is conducted using both SEM and metallographic imaging as well as confocal microscopy.

Figure 5a and b depict the SEM images along the cut surface. In the case of guillotine shear cutting, the percentage of the sheared surface amounts around 50% whereas the other half of the surface is fractured. This leads to different roughness values in the corresponding areas. While the roughness along the sheared surface is small (Figure 5b1), it rises on the fractured part (Figure 5b2). The surface after the water jet cutting is jagged (Figure 5b3) which is partly caused by a fast growing oxide layer due to the use of water as a cutting medium. It could not be removed without altering the surface roughness. In top view, no difference between topside and bottom can be detected.

The vicinity of the cross-section after shear cutting shows deformed grains (Figure 5c, left) and shear bands induced by cold deformation. Water jet cutting leads to a bigger burr and transcrystalline material separation (Figure 5c, right). Neither a grain deformation nor the appearance of shear bands can be determined after water jet cutting which confirms that water jet cutting is the smoother process.

3.2.2. Microhardness Measurements

Results of microhardness measurements HV 0.05 measured from the cut surface to the core are shown in **Figure 6**. Displayed are two measurements for each sample series: guillotine shear (RD) (TD) and water jet (RD) (TD). The core strength amounts to 242 ± 10 HV 0.05. For all

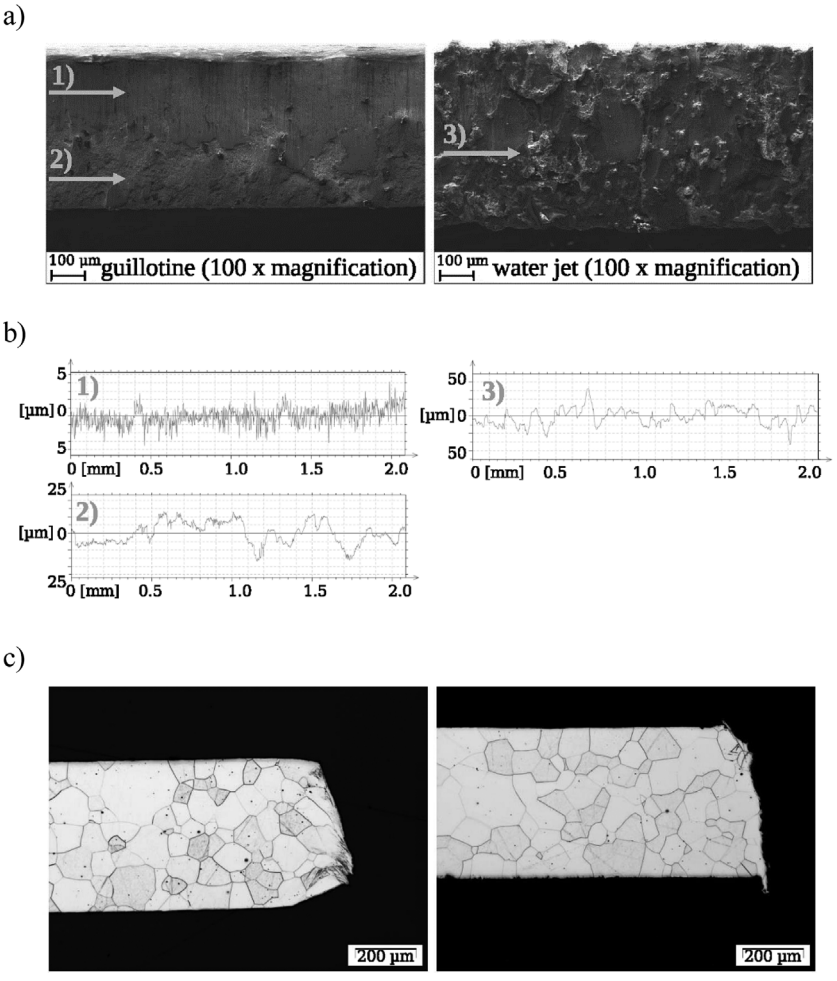

Figure 5. SEM image of the cut surface a), roughness of cut surface b), and metallographic image of sheet cross-section c), for guillotine shear (left column) and water jet cut samples (right column).

samples, cutting raises the hardness close to the cut surface. No difference in the hardness profile between RD and TD can be encountered. On the other hand, an influence of the different cutting processes is reflected in the microhardness. Guillotine shear cutting has a major effect on hardness which is represented by a maximum hardness of 400 HV 0.05 compared to 327 HV 0.05 by water jet cutting, measured in the sheet cross-section perpendicular to the cut surface in a distance of 22 µm from the cut surface. As a result of guillotine cutting, the area with increased microhardness compared to the core hardness is 100 µm deeper than after water jet cutting.

Due to hardening, it can be assumed that cutting causes stresses in the region close to the cut surface. The shear bands close to the cut surface, induced by guillotine cutting, indicate larger cold deformation and therefore higher stresses.

The stresses from water jet cutting are estimated to be lower compared to guillotine cut samples. Despite no visible influence on the microstructure of the water jet cut samples, a hardening near the cut surface can be measured nonetheless. A possible heating during water jet cutting, as a result of the abrasive particles, pressure and speed can be excluded because sample thicknesses are small. Therefore, temperature influence on the samples, as occurring during laser cutting can be excluded indicating solely mechanical originated, residual stresses as a result of water jet cutting.

3.2.3. Effect of Cutting on the Magnetic Properties

Figure 7 depicts hysteresis loops at 1.0 T and quasi-static excitation. For three sample series, an analogous behavior is observed. Guillotine shear cutting of the samples along rolling (RD) and transverse direction (TD) shows shearing of the hysteresis loop with increasing amount of cut surface per sample volume, see Figure 7a and b. Both the magnetization field strength as well as the coercive field strength increase, whereas the remanence decreases. Generally, samples cut in TD show larger hysteresis loop areas and require higher magnetization field strengths.

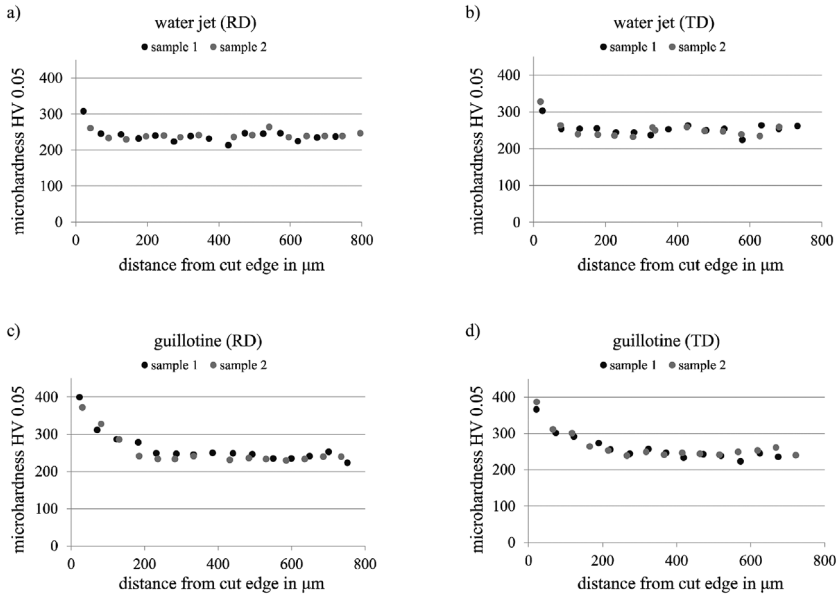

Figure 6. Microhardness measurements HV 0.05 with increasing distance from the cut surface for a), b) water jet cutting and c), d) guillotine shear cutting in a), c) rolling direction (RD) and b), d) transverse direction (TD).

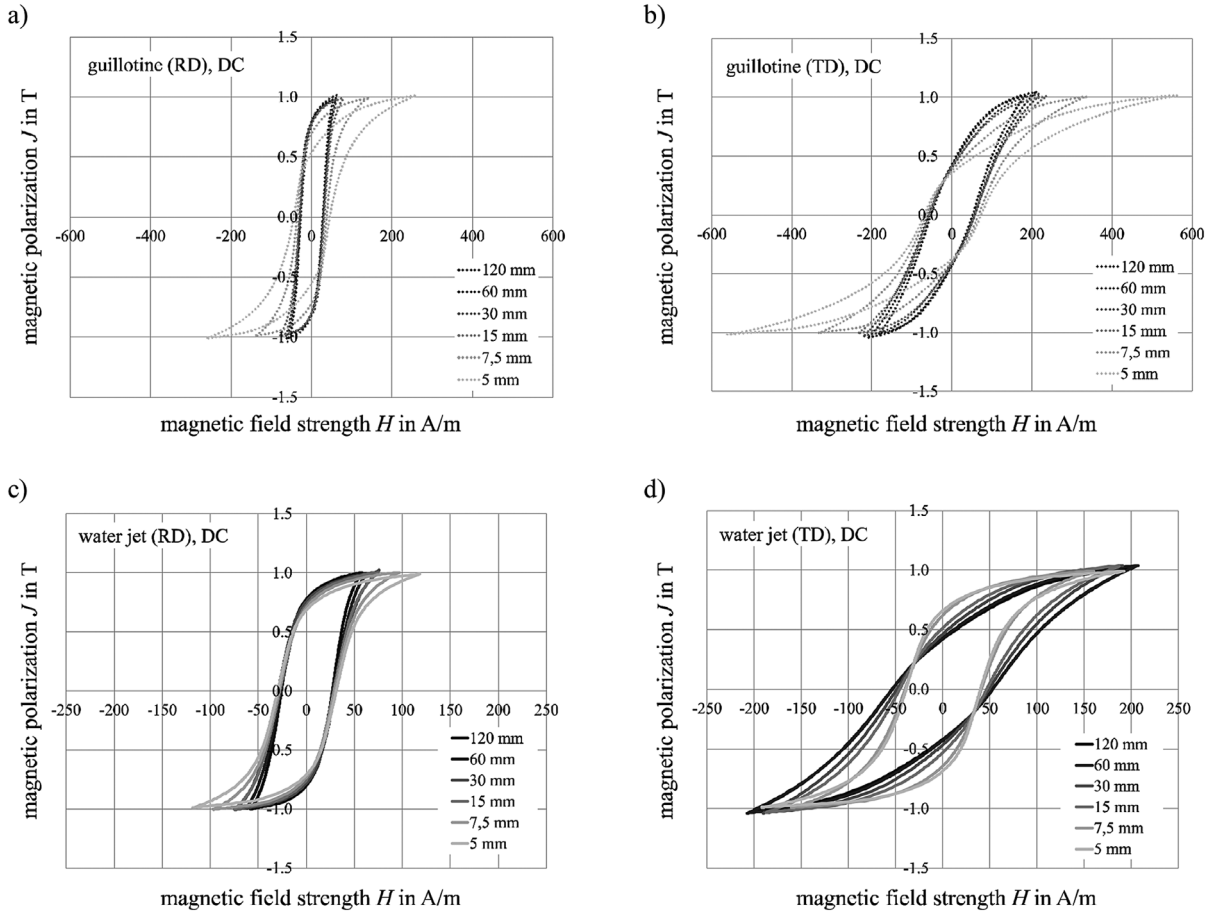

Figure 7. Quasi-static (DC) hysteresis loops at 1.0 T for different cutting techniques, sample directions, and increasing proportions of cut surface per initial sample volume. a) Guillotine shear cut, rolling direction, b) guillotine shear cut, transverse direction, c) water jet cut, rolling direction, and d) water jet cut transverse direction.

The shearing, e.g., change of the characteristic magnetic values is larger compared to RD. Water jet cutting in RD (Figure 7c) shows analogous shearing of the hysteresis curve with increasing amount of cut surface per sample volume. However, the deterioration is much less severe than with guillotine shear cutting.

In contrast, water jet cutting along TD leads to a completely different magnetic behavior. A slight improvement of magnetization with increased amount of cut surface per sample volume is observed with an increasing permeability leading to a steeper curve.

Closer investigation of the loss behavior further confirms the possible improvement for water jet cut samples in TD for certain excitations. In **Figure 8**, static and dynamic losses calculated from the quasi-static measurements and experimental results at different frequencies are displayed for three different excitations. The observations of the behavior of Figure 7 with three analogous sample series can be applied to losses for lower frequencies and polarizations. 50 Hz guillotine cut samples series in RD and TD, just as water jet cut samples RD, show increasing specific losses with an increasing amount of cut surface per volume, for each polarization. In contrast, water jet cut samples in transverse direction show decreasing losses with increasing cut surface per sample volume for polarizations of 0.5 T and 1.0 T. At higher polarizations of 1.5 T, specific losses increase. In each of these cases, specific losses show the same tendencies as the respective static losses but with smaller differences in dynamic losses for the different strip widths, indicating a larger influence of stresses on the hysteresis losses. For higher frequencies, the influence of dynamic losses increases. For the specimens cut by water jet in TD at 0.5 T and 400 Hz static and total losses decrease. At 1.0 T total losses increase even though static losses decrease. At 1.5 T and 400 Hz total losses increase and it is apparent that dynamic losses increase with an increasing amount of cut surface per sample volume.

The presented results indicate that water jet as well as guillotine cutting lead to residual stresses in the material. Microhardness measurements and a microstructural analysis, e.g., higher hardness close to the cut surface, a further mechanically influenced zone, shear bands, and a more severe deterioration of magnetic properties indicate

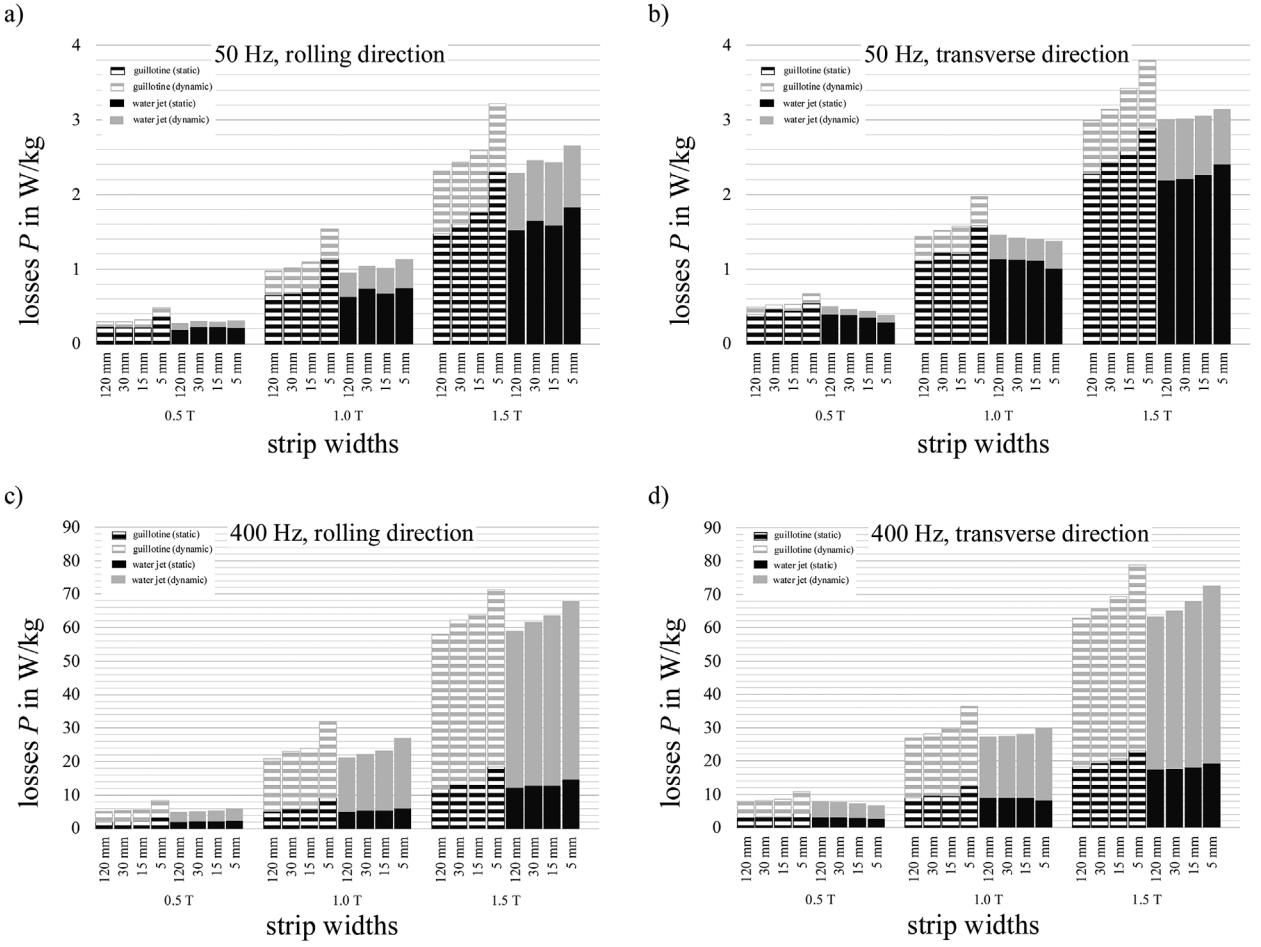

Figure 8. Influence of frequency, polarization, cutting technique, and strip width on the dynamic and static losses.

higher internal stresses resulting from guillotine cutting in comparison to water jet cutting. In TD, an improvement can occur if the induced stresses originating from the cutting method are below a specific value. In this way, the overall magnetic behavior can be improved by a rising number of cuts in TD. From the theoretical point of view, this observation might be caused by a combination of different effects, some of which have briefly been discussed in Section 3.1.

Processing can cause misorientations in the mechanically influenced area. Linked to the domain theory, this could lead to a different distribution of magnetic domains which might simplify their rotation along the external applied field during magnetization process.

Moreover, the anisotropy of magnetostriction should be taken into account. If the external field and the applied stresses are collinear, it will facilitate the magnetization process in case of positive magnetostriction which is found in the [100] direction. Between [100] and [111] directions, magnetostriction changes its values from positive to negative depending on the magnetic field strength which might explain why the observed magnetic improvement occurs as a function of polarization.[32] The actual influence of stresses on the magnetostriction constants and change of the global anisotropy of the magnetostriction as a result of the alignment of grains are yet to be identified.

Finally, a favorable combination of grain orientations, magnetic domains, magnetostriction, and applied stresses might be an explanation for the magnetic behavior along TD for the discussed limited value range of polarization, frequency, tensile stress, and strip width. Because of the limited value range, a direct practical benefit of this effect seems to be improbable. Moreover, for non-grain-oriented electrical steels, isotropic electromagnetic properties are desired to ensure an evenly distributed magnetic behavior in rotating machines and the improvement of the magnetic flux in one direction of the electrical steel sheet might harm the flux in the other directions.

In order to optimize non-grain-oriented electrical steel with regard to its application in rotating electrical machines, the microstructural- and stress-related changes of electromagnetic properties in FeSi steels need to be studied and understood. The results for the investigated material enable correlations between the material, the processing, and its application with regard to different interdependence levels. The presented findings show the importance of considering rolling and transverse direction when studying effects on electrical steel. NGO is ought to have isotropic magnetic behavior to ensure a homogenous isotropic magnetic field in all spatial directions at all rotational angles. The results showed the effect of anisotropy on the magnetic properties was considerable. Consequently, this shows that today's modeling and design of electrical machines, with its simplifications regarding the description of magnetic material behavior with neglect of anisotropic effects as well as disregard of mechanical processing, is insufficient. Furthermore, the results introduce the potential of possible beneficial effects of stresses on the magnetic properties for electromagnetic applications which need to be considered in simulation tools. In order to include these effects in modern day machine modeling, the phenomenology and appropriate quantification methods need to be conducted. However, other vital correlations need to be discussed in further studies, especially the influence of stress on intrinsic material properties such as magnetostriction or crystalline anisotropy in order to explain the behavior of smaller stresses.

4. Conclusions

Based on the results above, it may be concluded that

1. Cutting by guillotine compared to cutting by water jet is more detrimental to the magnetic properties of high-silicon steel.
2. If mechanical stress is applied parallel to the rolling direction with the same magnetic flux direction during magnetic measurements, increased losses and sheared hysteresis loops can be observed.
3. If tensile stress is applied in transverse direction, the influence is more complex compared to the behavior in rolling direction. For small tensile stresses, in this study to about 50 MPa, the magnetization improves compared to the unloaded state with minimum required magnetization field strength for about 10 MPa tensile stress and given low polarizations and frequencies.
4. An improvement of magnetic properties can also be observed with a rising number of cuts performed by water jet. The beneficial effects on magnetic properties depend on polarization, frequency, orientation of the specimen in the sheet plane and test direction.

Acknowledgements

The work of N. Leuning and S. Steentjes is supported by the DFG and carried out in the research group project "Low-Loss Electrical Steel for Energy-Efficient Electrical Drives" and as part of the research project "Improved modeling and characterization of ferromagnetic materials and their losses." M. Schulte and W. Bleck would like to thank company C.D. Wälzholz for their support and the material staging.

Received: February 4, 2016; Revised: April 12, 2016

Keywords: electrical steel; soft magnetic property; material processing; cutting edges; internal mechanical stress

References

[1] A. J. Moses, *Scr. Mater.* **2012**, *67*, 560.
[2] P. Ghosh, R. R. Chromik, A. M. Knight, S. G. Wakade, *J. Magn. Magn. Mater.* **2014**, *356*, 42.
[3] M. F. Littmann, *IEEE Trans. Magn.* **1971**, *7*, 48.
[4] P. Brissonneau, *J. Magn. Magn. Mater.* **1984**, *41*, 38.
[5] J. K. Stanley, *Metallurgy and Magnetism*, American Society for Metals, Ohio, USA **1949**.
[6] K. Jenkins, M. Lindenmo, *J. Magn. Magn. Mater.* **2008**, *320*, 2423.
[7] D. S. Petrovic, B. Markoli, M. Ceh, *J. Magn. Magn. Mater.* **2010**, *322*, 3041.
[8] E. T. Stephenson, A. R. Marder, *IEEE Trans. Magn.* **1986**, *22*, 101.
[9] H. Shimanaka, Y. Ito, K. Matsumura, B. Fukuda, *J. Magn. Magn. Mater.* **1982**, *26*, 57.
[10] K. Matsumura, B. Fukuda, *IEEE Trans. Magn.* **1984**, *20*, 1533.
[11] O. Kypris, I. C. Nlebedim, D. C. Jiles, *J. Appl. Phys.* **2014**, *115*, 17E305.
[12] J. Schneider, A. Franke, A. Stöcker, R. Kawalla, *Steel Res. Int.* **2016**, doi: 10.1002/srin.201500447.
[13] W. M. Arshad, T. Ryckebush, F. Magnussen, H. Lendenmann, J. Soulard, B. Eriksson, B. Malmros, *Conference Record of the 2007 IEEE Industry Applications Conference 2007*, New Orleans, LA, USA *2007*, 94.
[14] A. J. Clerc, A. Muetze, *IEEE Trans. Ind. Appl.* **2012**, *48*, 1344.
[15] E. Araujo, J. Schneider, K. Verbeken, G. Pasquarella, Y. Houbaert, *IEEE Trans. Magn.* **2010**, *46*, 213.
[16] M. Emura, F. J. G. Landgraf, W. Ross, J. R. Barreta, *J. Magn. Mag. Mater.* **2003**, *254*, 358.
[17] Y. Kurosaki, H. Mogi, H. Fujii, T. Kubota, M. Shiozaki, *J. Magn. Magn. Mater.* **2008**, *320*, 2474.
[18] R. Siebert, J. Schneider, E. Beyer, *IEEE Trans. Magn.* **2014**, *50*, 1.
[19] A. Schoppa, J. Schneider, C. D. Wuppermann, *J. Magn. Magn. Mater.* **2000**, *215*, 74.
[20] T. Belgrand, S. Eple, *J. Phys. IV* **1998**, *8*, 611.
[21] E. Hug, O. Hubert, J. J. Van Houtte, *Mater. Sci. Eng.* **2002**, *332*, 193.
[22] V. Permiakov, L. Dupré, A. Pulnikov, J. Melkebeek, *J. Magn. Magn. Mater.* **2004**, *272–276*, E553.
[23] C. S. Schneider, *J. Appl. Phys.* **2005**, *97*, 10E503.
[24] T. Nakata, M. Nakano, K. Kawahara, *IEEE Trans. J. Magn.* **1992**, *7*, 453.
[25] S. Krupička, *Physik der Ferrite und der verwandten magnetischen Oxide*, Vieweg, Braunschweig, Germany **1973**, Ch. 4.
[26] B. D. Cullity, C. D. Graham, *Introduction to Magnetic Materials*, John Wiley & Sons, Inc., Hoboken, NJ, USA **2008**, Ch. 7.
[27] R. M. Bozorth, *Ferromagnetism*, IEEE Press, New York **1993**.
[28] V. E. Iordache, E. Hug, N. Buiron, *Mater. Sci. Eng.* **2003**, *359*, 62.
[29] C. G. Stefanita, L. Clapham, D. L. Atherton, *J. Mater. Sci.* **2000**, *35*, 2675.
[30] J. M. Makar, B. K. Tanner, *J. Magn. Magn. Mater.* **2000**, *222*, 291.
[31] R. Becker, W. Döring, *Ferromagnetismus*, Springer-Verlag, Berlin/Heidelberg, Germany **1939**.
[32] G. Bertotti, F. Fiorillo, in *Landolt-Börnstein: Numerical Data and Functional Relationships in Science and Technology*, Vol. *19i1* (Ed: H. P. J. Wijn), Springer-Verlag, Berlin/Heidelberg, Germany **1994**, pp. 33–143.